Static and Dynamic Light-Scattering Studies on Semidilute Solutions of Polystyrene in Cyclohexane as a Function of Temperature

Taco Nicolai and Wyn Brown*

Institute of Physical Chemistry, University of Uppsala, Box 532, 751 21 Uppsala, Sweden

Received October 24, 1989

ABSTRACT: Static and dynamic light-scattering measurements have been made on semidilute solutions of a high molecular weight polystyrene sample in cyclohexane in the temperature range 29–65 °C. The results are compared to mean-field and scaling theory. A more consistent agreement with mean-field theory is found over the whole temperature range investigated. The effect of topological constraints on the autocorrelation function of the scattered light is investigated as a function of temperature and is found to become less important with increasing temperature. The influence of topological constraints on the cooperative diffusion coefficient is rather well described by a theory of Brochard and de Gennes.

Introduction

Over the last decade various scattering techniques have been employed to investigate static and dynamic properties of semidilute solutions of linear polymers. For good solvents the experimental results can be well explained by scaling theory[1,2] or more general renormalization group theories.[3,4] On the interpretation of results from experiments on poor and marginal solvent systems, there still exists some controversy.

The effect of solvent quality may be studied by varying the temperature in a poor solvent system. By increasing the temperature from the Θ temperature, one can go from a system where binary thermodynamic interactions are effectively nonexistent to a system where they are dominant. The experimental results of such studies have usually been interpreted in terms of either or both scaling theory and mean-field theory. It turns out that temperature and concentration dependences of static properties like the inverse osmotic compressibility, $\delta\pi/\delta C$, and the static correlation length, ξ_s, are consistent with both of the two theoretical approaches over a wide range of temperatures. For example, $\delta\pi/\delta C$ data obtained from static light scattering (SLS)[5] and ξ_s data from small-angle neutron scattering (SANS)[6] experiments on semidilute solutions of polystyrene in cyclohexane at temperatures between 35 °C (Θ temperature) and 65 °C have been successfully explained in terms of both Daoud and Jannink's scaling theory [5,6,7] and Moore's mean-field theory.[8,9] The same experimental data have also been analyzed in terms of renormalization group theories, which were extended to include the effect of ternary interactions. In one case,[10] on the basis of the SLS data, it was concluded that the limiting good solvent scaling behavior is reached early in the investigated temperature range. In another case,[3] on the basis of the SANS data, it was concluded that such a limiting scaling behavior is not reached even at 65 °C. Schaefer et al.[11,12] considered the effect of chain stiffness and concluded that for semiflexible polymers like polystyrene mean-field theory is appropriate for marginal solvent systems. They suggest that the good solvent scaling law behavior, which has been reported for semidilute solutions of polystyrene in cyclohexane within the temperature range 35–60 °C, is only apparent. A similar conclusion has been drawn recently by Kinugasa et al.[13] on the basis of an extensive study on the concentration and temperature dependence of ξ_s and $\delta\pi/\delta C$ of semidilute polystyrene solutions in cyclohexane. Although their data can be fitted to power laws, on the whole, the results are deemed more consistent with mean-field theory.

The dynamic behavior as studied by dynamic light scattering (DLS) is complicated by the effect of topological constraints on the movement of the polymer chains, which do not influence static properties as they are not permanent, and all chain conformations are accessible. These constraints, which lead to temporary entanglements, influence the cooperative diffusion coefficient, D_c, and thus the value of the effective dynamic correlation length, which is usually calculated as

$$\xi_e = kT/6\pi\eta D_c \tag{1}$$

where k is the Boltzmann constant and η the viscosity of the solvent at temperature T. In addition they give rise to slow modes in the autocorrelation function of the scattered light. At Θ conditions the effect of topological constraints on the autocorrelation function has been described by a theory by Brochard and de Gennes.[14,15] Recent DLS experiments on semidilute solutions of polystyrene at Θ conditions confirm the main features of their theory, but the viscoelastic properties of the transient network are found to be more complicated than they assumed.[16,17] The influence of topological constraints on the autocorrelation function decreases with increasing solvent quality due to the increasing dominance of thermodynamic interactions and is probably negligible in good solvents. An additional complication arises due to the fact that, even if the effect of topological constraints is ignored, the dynamic and static correlation lengths are not necessarily proportional, as the first length scale characterizes hydrodynamic screening and the second excluded-volume screening.[18] Furthermore, a different type of averaging over length scales is involved in static and dynamic measurements.[19–21] To our knowledge, only one systematic study of the temperature dependence of the cooperative diffusion coefficient of semidilute solutions in a Θ solvent has been conducted.[22] In this study, however, the diffusive mode was not separated from the slow modes nor was the effect of topological constraints on the value of D_c taken into account. This neglect invalidates the conclusions drawn from these measurements, as is the case for most earlier DLS studies of semidilute solutions in poor and marginal solvents.

In the following we will present results from static and

0024-9297/90/2223-3150$02.50/0

Table I
Experimental Values of $(\delta\pi/\delta C)/(RT) \times 10^3$ at Various Temperatures and Concentrations

	$C \times 10^2$, g·mL^{-1}			
T, °C	12.6	10.2	3.7	3.0
65	11.0	8.0	2.1	1.5
60	9.4	7.0	1.7	1.2
55	8.7	6.4	1.5	1.1
50	6.9	5.2	1.1	0.89
45	5.5	4.0	0.89	0.65
40	4.5	3.0	0.59	0.48
35	3.0	2.0	0.27	0.21
33	2.5	1.5	0.17	0.13

dynamic light-scattering measurements on semidilute solutions of polystyrene ($M_w = 3.8 \times 10^6$) in cyclohexane over a range of temperatures between a few degrees below Θ and 65 °C. At each temperature a number of concentrations between 3 and 12.6% have been measured. The results will be compared with predictions from scaling and mean-field theory. Furthermore, we will extend our earlier study of the slow modes on the autocorrelation curve at Θ conditions by looking at the effect of temperature and thus solvent quality on these modes.

Experimental Section

Polystyrene solutions were prepared using polymers from Toya Soda Ltd., Japan: $M_w = 3.8 \times 10^6$, $M_w/M_n = 1.05$. The solvent was spectrograde cyclohexane from Merck, Darmstadt, FRG, and was used without further purification except for drying over 3-Å molecular sieves. The solutions were made by dissolution of the polymer in cyclopentane followed by centrifugation. The upper portion was used, and the cyclopentane was evaporated and replaced by a measured amount of filtered cyclohexane in the measuring cell, which was then flame-sealed. The solutions were allowed to mature for months prior to use. Concentrations were calculated from the weight fraction, W, using $C = \rho W$, where $\rho = 0.764$ is the density of the solution at 35 °C. Using a single value for ρ for all temperatures and concentrations introduces only a small error in the value C.[23]

The apparatus used to check the angular dependence of the time-averaged intensity of the scattered light has been described elsewhere.[24] Subsequent SLS measurements were performed at a scattering angle of 90° on the same equipment used for the DLS measurements; see for details of the experimental arrangement ref 25. The light source was in both cases a 632-nm He–Ne laser. For the DLS measurements an ALV-Langen Co., multibit, multi-τ autocorrelator was operated with 23 simultaneous samplings (covering, for example, delay times in the range 1 μs to 1 min) in the logarithmic mode and 191 channels.

Results

Static Light Scattering. For all samples the angular dependence of the Rayleigh ratio, R_{90}, was checked by measuring the intensity at various scattering angles between 50 and 100°. No systematic dependence of R_{90} was observed, which means that the influence of intra- and intermolecular interference of the scattered light may be neglected here and R_{90} is related to the inverse osmotic compressibility by[26]

$$\frac{KC}{R_{90}} = \frac{1}{RT}\frac{\delta\pi}{\delta C} \tag{2}$$

where $K = 4\pi^2 n_0^2 (\delta n/\delta C)^2 / N_A \lambda^4$, n_0 is the refractive index of the solvent, $\delta n/\delta C$ is the refractive index increment, λ is the wavelength of the light, N_A is Avogadro's number, and R is the gas constant. The experimental values of $(\delta\pi/\delta C)/(RT)$ are given in Table I. The errors in the individual data depend on the concentration and the temperature and are estimated to become as large as 20%. Results from similar measurements on semidilute solutions of polystyrene in cyclohexane reported by Štěpánek et al.[5] show the same uncertainty. This relatively large error is probably due to the slow intensity fluctuations that occur in semidilute polymer solutions at temperatures close to Θ.

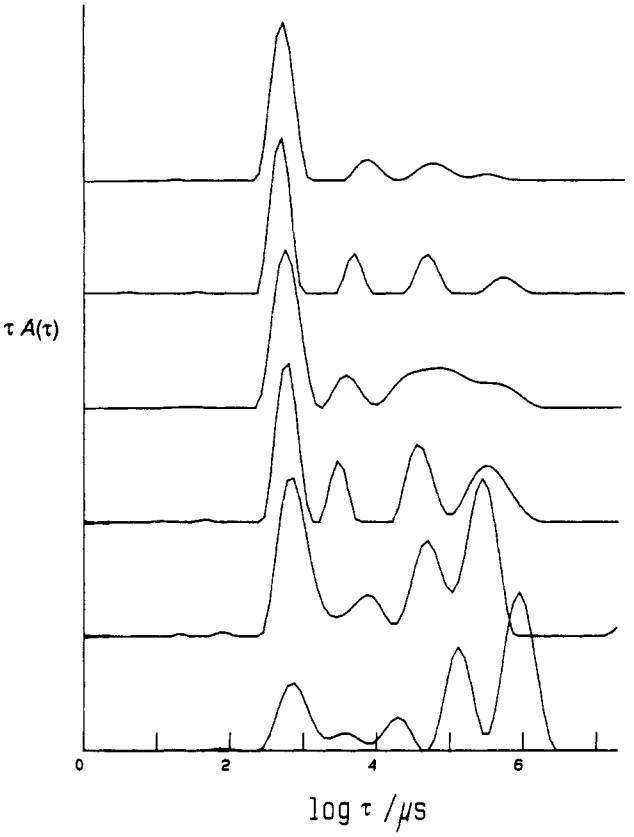

Figure 1. Relaxation time distributions obtained using REPES, of semidilute solutions of polystyrene in cyclohexane ($M_w = 3.8 \times 10^6$, $C = 6.4 \times 10^{-2}$ g·mL^{-1}, $q^2 = 4.0 \times 10^{-14}$ m^{-2}) for different temperatures. From bottom to top, T = 31, 35, 37, 40, 50, and 60 °C. The distributions are reduced to Θ temperature by multiplying the time axis by $(T\eta_\theta/308\eta_T)$ with T in Kelvin.

The correlation curves obtained from DLS measurements were analyzed by performing an inverse Laplace transformation using a constrained regularization calculation program called REPES[27] to obtain the distribution $A(\tau)$ of relaxation times; see ref 16 for a description of the analysis method. A broad distribution of relaxation times was obtained for all samples at most temperatures. The dependence of these relaxation time distributions on the scattering vector, q, and the polymer concentration at the Θ temperature has been treated elsewhere.[16] Here we will concentrate on the temperature dependence. In Figure 1 relaxation time distributions are shown for one sample ($C = 0.067$ g/mL) at various temperatures between 31 °C, which is just above the phase separation temperature, and 60 °C. As expected the relative amplitude of the sum of the slow modes, A_s, decreases with increasing temperature; see Figure 2. However, the contributions of the slow modes do not decrease at equal rate; the slowest mode decreases more strongly. The relaxation rate, Γ, characterizing the fast mode is q^2-dependent at all temperatures. The cooperative diffusion coefficient was calculated from this relaxation rate by using $\Gamma_c = D_c q^2(1-\phi)$ where the factor $1-\phi$ is included to correct for backflow due to the finite volume fraction of the polymer, ϕ. Using eq 1 values of the effective dynamic correlation length, ξ_e, were obtained, which are tabulated in Table II. The error in these values is estimated to be less than 5%. The solvent viscosities used

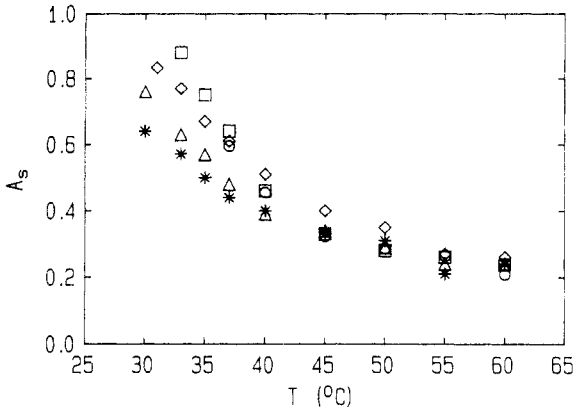

Figure 2. Plot of the relative amplitude of the sum of the slow modes as a function of the temperature for various concentrations: C = 3.0 (○), 3.7 (□), 6.4 (◇), 10.2 (▲), 12.6 × 10^{-2} g·mL^{-1} (*).

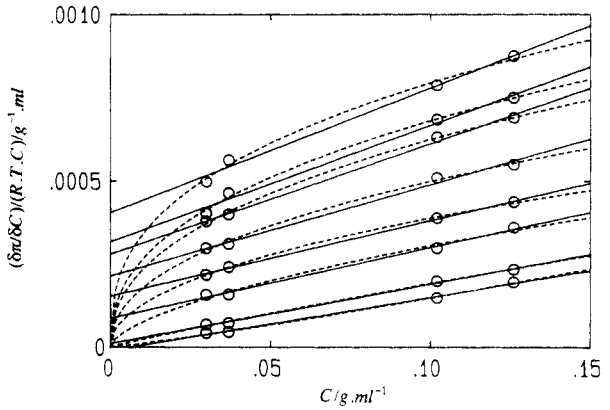

Figure 3. Plot of $(\delta\pi/\delta C)/(RTC)$ as a function of the concentration for various temperatures. From bottom to top, T = 33, 35, 40, 45, 50, 55, 60, and 65 °C. The broken lines are nonlinear mean least-squares fits to $y = aC^x$ representing scaling behavior, and the solid lines are linear mean least-squares fits representing mean-field behavior.

Table II
Values of the Effective Dynamic Correlation Length in Angstroms at Various Temperatures and Concentrations

	$C \times 10^2$, g·mL^{-1}				
T, °C	12.6	10.2	6.4	3.7	3.0
60	59	67	82	118	146
55	60	73	92	120	153
50	70	79	104	133	159
45	82	89	117	156	187
40	93	102	131	178	210
37	104	116	140	193	234
35	121	130	175	230	
33	123	138	192		
30	137	152			
29	148				

in the calculation of ξ_e have been measured at each temperature and agree well with the empirical relation given in ref 28.

Discussion

We will use two different theoretical approaches to interpret the experimental results. The first one uses a mean-field approximation for the thermodynamic interactions between the polymer chains, which leads to the following expressions for the osmotic compressibility and the static correlation length:[8,29]

$$\frac{1}{RT}\frac{\delta\pi}{\delta C} = N_A B_1 C + 3N_A^2 B_2 C^2 \tag{3}$$

$$\xi_s^{-2} = 12\frac{N_A}{a^2}B_1 C + 36\frac{N_A^2}{a^2}B_2 C^2 \tag{4}$$

Here B_1 and B_2 are interaction parameters characterizing binary and ternary thermodynamic interactions, respectively. $a = \sqrt{6}R_g/M^{0.5}$ with R_g the unperturbed radius of gyration and M the molecular weight of the polymer chains (for polystyrene $a \approx 0.7$ Å[30]). A constant term containing M^{-1}, which is negligible for the high molecular weight sample used here, has been left out of both equations.

An alternative approach is a scaling theory developed by Daoud and Jannink.[7] They introduced a concentration–temperature diagram, which for semidilute solutions is divided into two regions with a boundary at $\tau = \tau^{**} \sim C$, where $\tau \equiv (T - \theta)/T$ is the reduced temperature. For $(\delta\pi/\delta C)/(RTC)$ and ξ_s the following scaling relations are given

$$\frac{1}{RT}\frac{\delta\pi}{\delta C} \sim C^2 \quad \tau < \tau^{**}$$
$$\sim C^\alpha \tau^\beta \quad \tau > \tau^{**} \tag{5}$$
$$\xi_s^{-1} \sim C \quad \tau > \tau^{**}$$
$$\sim C^\gamma \tau^{1-\gamma} \quad \tau > \tau^{**} \tag{6}$$

where α, β, and γ are 1.25, 0.75, and 0.75, respectively, when the excluded-volume exponent, ν, is 0.6 and 1.31, 0.69, and 0.77 when ν = 0.588. Schaefer et al.[11,12] modified this theory for semiflexible chains, introducing a third so-called marginal solvent region for which mean-field theory is supposed to be valid. Scaling relations are recovered from eqs 3 and 4 by assuming $B_1 \gg N_A B_2 C$ for the marginal solvent region and $B_1 \ll N_A B_2 C$ for the poor solvent region. At the Θ-temperature both theoretical approaches give the same concentration dependence as B_1 is zero in this case.

Equations 4 and 6 are derived for the static correlation length. If one wants to apply these equations to the dynamic correlation length, one has to assume that ξ_e is simply proportional to ξ_s. This may be correct in the good solvent limit where the effect of topological constraints on D_c is very small, but it is certainly not the case for Θ systems.

Static Light Scattering. In Figure 3 values of $(\delta\pi/\delta C)/(RTC)$ are shown as a function of the polymer concentration for various temperatures between 33 and 65 °C. Scaling theory predicts that these values vary with C^x, see eq 5, where x changes from 1 at temperatures close to Θ to 0.25 for $\tau \gg \tau^{**}$. The dashed lines through the data represent least-squares fits to such a scaling relation. The values of x are found to decrease gradually from 1.15 at 33 °C via 0.9 at 35 °C to 0.37 at 65 °C. On the other hand, following mean-field theory, $(\delta\pi/\delta C)/(RTC)$ is expected to increase linearly with the polymer concentration at all temperatures with a slope determined by B_2 and an intercept determined by B_1. Values of B_1 and B_2 determined from linear least-squares fits (solid lines in Figure 3) are plotted versus τ in Figure 4. Both B_1 and B_2 show a linear increase over the whole temperature range investigated

$$B_1 = 7.0 \times 10^{-27}\tau + 0.3 \times 10^{-28}\ \text{cm}^3 \tag{7}$$
$$B_2 = 2.1 \times 10^{-50}\tau + 1.6 \times 10^{-51}\ \text{cm}^3$$

where the small residual value of B_1 at $\tau = 0$ is probably within the measurement error. Interestingly, if this interpretation of the data is correct, it would follow that ternary thermodynamic interactions increase, albeit mod-

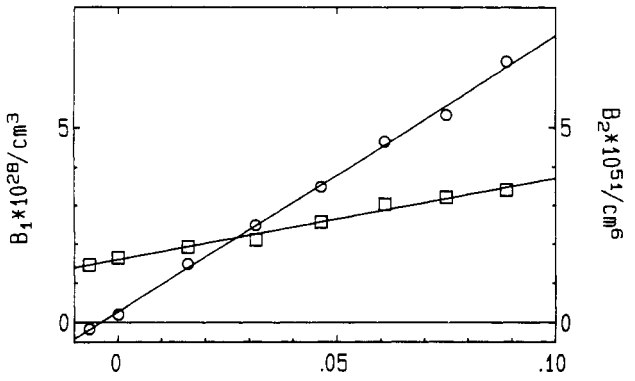

Figure 4. Plot of the parameters B_1 (circles) and B_2 (squares) in eq 7 as a function of the reduced temperature.

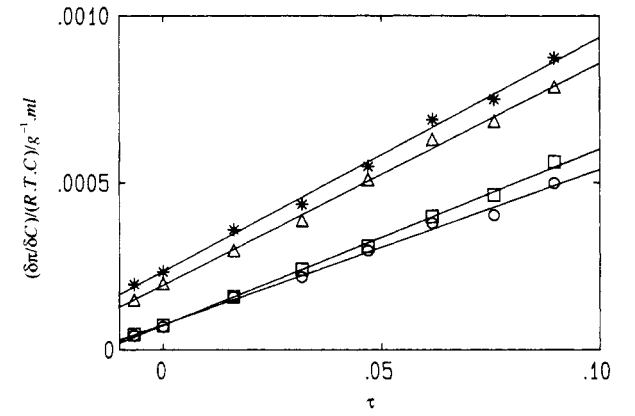

Figure 5. Plot of $(\delta\pi/\delta C)/(RTC)$ as a function of the reduced temperature for various concentrations. Symbols are the same as in Figure 2.

erately, with increasing temperature, which is contrary to what is usually assumed in literature but agrees with observations of Vink[31] on the same system. The absolute values of B_1 are close to those obtained from SANS and SAXS measurements on the same system[9,13,19,32] while the values of B_2 are somewhat larger. It appears from Figure 3 that over the limited range of concentrations measured both a linear and an exponential fit are equally justified by the data. For an objective distinction between the two approaches, far more accurate data are necessary, which will be difficult to achieve in practice, or the range of concentrations must be extended toward lower concentrations. The latter can be obtained by using higher molecular weight samples for which the semidilute regime is reached at lower concentrations. Extending the concentration range to higher concentrations would mean that system is no longer semidilute. The results presented here are consistent with both eqs 3 and 5. However, no constant limiting value for the exponent is reached within the temperature range investigated here as might be expected from scaling theory.

In Figure 5 the temperature dependence of $(\delta\pi/\delta C)/(RTC)$ is shown for each concentration. At all concentrations investigated $(\delta\pi/\delta C)/(RTC)$ increases linearly with increasing temperature, and, clearly, there is no indication for the existence of distinct regimes. The linear increase can be explained in terms of mean-field theory, however, if both B_1 and B_2 are taken to increase linearly with temperature. This agrees with the results obtained from the concentration dependence; see Figure 4. In fact, a careful analysis of the temperature dependence yields relationships for B_1 and B_2 that are very close to those obtained from the concentration dependence given in eq 7. Sometimes osmotic compressibility data are presented in the form of a universal curve by plotting $(\delta\pi/\delta C)/(RTC^2)$ versus τ/C;[5,13] see Figure 6. A universal curve is expected for such a plot from scaling theory as $\tau^{**} \sim C$ and $(\delta\pi/\delta C)_\theta \sim C^2$. Within mean-field theory a universal curve is obtained if B_2 is independent of the temperature. It is clear from Figure 6 that universal behavior is obtained only approximately as might be expected from the slight temperature dependence of B_2. The solid and dashed line through the data are obtained from a linear and an exponential fit representing the expected behavior according to mean-field theory and scaling theory in the good solvent limit, respectively. In the latter case an exponent of 0.67 is found if it is assumed that the good solvent regime is reached for $\tau/C > 0.5$, which is close to the value reported by Štěpánek et al.[5] Again we find that both approaches describe the data equally well, at least for $\tau/C > 0.5$, but considering the whole temperature range, an exponential fit over a limited range of τ/C seems arbitrary as there is no indication for the existence of different regimes.

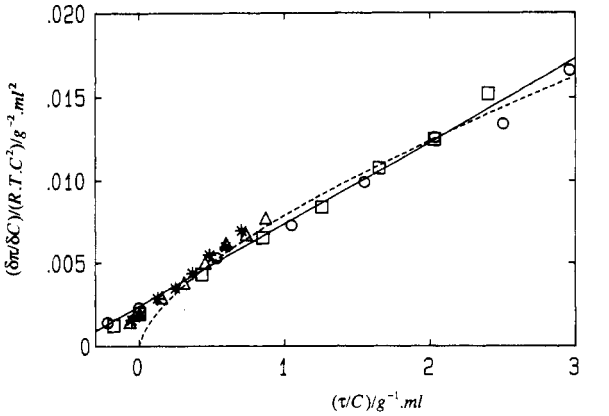

Figure 6. Plot of $(\delta\pi/\delta C)/(RTC^2)$ as a function of τ/C. Symbols are the same as in Figure 2. The broken line is a nonlinear mean least-squares fit to $y = aC^x$ for $\tau/C > 0.5$ representing good solvent scaling behavior, and the solid line is a linear mean least-squares fit representing mean-field behavior.

In summary the SLS measurements do not support scaling theory and are consistent with mean-field theory over the concentration and temperature range investigated. However, accurate data over a wider range of concentrations are necessary in order to establish conclusively whether $(\delta\pi/\delta C)/(RTC)$ really increases linearly with concentration and to obtain accurate values of B_1 and B_2.

Dynamic Light Scattering. The DLS results cannot be directly interpreted in terms of either of the two discussed theories as they both neglect the effect of topological entanglements. For semidilute polymer systems at Θ conditions Brochard and de Gennes developed a theory that describes the influence of topological entanglements on the intensity autocorrelation function of the scattered light.[14,15] According to this theory the autocorrelation function is a sum of two exponential decays, viz., a fast, q^2-dependent mode due to cooperative diffusion and a relatively slow, q-independent mode related to the disentangling of the transient network formed by topological entanglements. The main features of this theory have been confirmed by DLS measurements on polystyrene at Θ conditions.[16,17] However, instead of one slow mode, a broad distribution of q-independent slow modes is found. The exact nature of the origin of these modes is not known at present, but there are strong indications that they are closely related to the viscoelastic properties of the transient network. These indications follow from parallel studies on semidilute solutions of polystyrene in dioctyl phthalate, which is a Θ system at 22 °C,

involving both DLS and dynamical mechanical measurements.[33] In both cases broad distributions of relaxation times are obtained over almost identical time ranges, which extend in the same way with increasing concentration and molecular weight. Furthermore, it appears that also in the case of dynamical mechanical measurements the relative amplitude of the slowest part of the relaxation time distribution decreases with increasing temperature, even though the relative amplitudes of the individual slow modes are quite different between the two methods. A detailed account of the comparison between these two experimental methods will be given elsewhere.[33b] The relative contribution of the combined slow modes to the autocorrelation curve is expected to decrease when the thermodynamic interactions increase in strength, i.e., with increasing temperature and concentration, which is in agreement with the experimental results; see Figure 2. However, even at 60 °C their contribution is still about 25%. For the lowest two concentrations investigated here the slowest mode dominates at temperatures below θ. The relaxation time characterizing this mode is no longer independent of the scattering angle but becomes increasingly q-dependent when the temperature is decreased toward the phase-separation temperature, which is about 32 °C for these concentrations. A similar irregular q-dependence has been observed at the Θ-temperature at even lower concentrations and is probably due to an increasing influence of a slow diffusive process possibly caused by self-diffusion or critical fluctuations. No such q-dependence was observed for the higher concentrations even at temperatures slightly above the phase-separation temperature.

Following Brochard and de Gennes' theory,[14,15] the cooperative diffusion coefficient obtained from the fast mode may be written as the sum of two terms. One term reflects the contribution of the osmotic force in the response of the system to spontaneous concentration fluctuations, which would be the sole contribution if topological constraints did not occur. The other term describes the effect of the elastic force of the transient network formed by topological entanglements. The following relation for the effective dynamic correlation length is obtained:

$$1/\xi_e = 1/\xi_h + f/a \tag{8}$$

Here ξ_h is the hydrodynamic correlation length of the system if topological constraints are absent, f is the number of effective entanglements per binary contact, and a is the size of the monomer. It is ξ_h that is assumed to be proportional to ξ_s and to which the mentioned theories should be applied. At the Θ temperature the following empirical relation has been obtained:[16]

$$1/\xi_e = 4.5 \times 10^6 C + 2.6 \times 10^5 \text{ cm}^{-1} \tag{9}$$

The first term on the right-hand side was identified as ξ_h^{-1} by comparison with classical gradient measurements[34] for which the effect of topological constraints can be neglected. Comparison with an empirical relation between ξ_s^{-1} and C at the Θ temperature from ref 13 shows that ξ_h and ξ_s are indeed proportional with $\xi_h/\xi_s \approx 2.7$. By implication the second term may be attributed to the effect of topological constraints. In order to investigate the relationship between a ξ_h and ξ_s at other temperatures, ξ_s values were calculated using experimental relationships given in ref 13. (Using other reported experimental values for ξ_s causes only small quantitative changes.) In Figure 7 all experimental values of ξ_e^{-1} are plotted as a function of their respective ξ_s^{-1} values. It appears that with the possible exception of the lowest concentration, a universal curve is obtained in this way. For $\xi_s^{-1} > 0.015$ Å^{-1}, ξ_e becomes proportional to ξ_s with $\xi_e/\xi_s = 1.7$. This value for ξ_e/ξ_s is close to those found in good solvents.[35] The fact that the data for $\xi_s^{-1} > 0.015$ Å^{-1} are well described by straight line through the origin implies that either the second part of eq 8 becomes proportional to ξ_s or that its contribution becomes negligible and $\xi_e \approx \xi_h$. The second option is most probable since ternary interactions influence the value of ξ_s while topological constraints are due to binary interactions only. For small values of ξ_s^{-1} there is a clear deviation from a simple proportionality. Extrapolation to $\xi_e^{-1} \approx 0.0026$ Å^{-1} at $\xi_s^{-1} = 0$ as expected from eq 9 seems quite reasonable in spite of the increased scatter in the data at smaller ξ_s^{-1} values. The general features of Figure 7 thus support the idea that D_c as measured by DLS consists of two parts. One part is due to the osmotic compressibility of the system and may be expressed in terms of a hydrodynamic correlation length, which is proportional to ξ_s, at least for the high molecular weight sample used here. The other part is due to topological constraints. The relative contribution of the first part increases with increasing temperature and concentration and becomes dominant at large values of ξ_s^{-1}, while the second part is dominant a small values of ξ_s^{-1}.

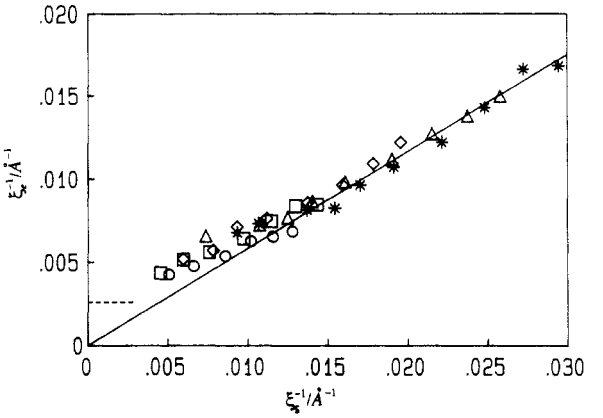

Figure 7. Plot of ξ_e^{-1}, as a function of ξ_s^{-1}. The solid line is a linear mean least-squares fit for $\xi_s^{-1} > 0.15$. The limiting value for ξ_e^{-1} at $\xi_s^{-1} = 0$ found for the Θ system (see eq 9) is indicated by the broken line.

Conclusion

The temperature and concentration dependences of the osmotic compressibility of semidilute solutions of polystyrene in cyclohexane are found to be consistent with Moore's mean-field theory in the temperature range 33–65 °C. Fitting to power laws, predicted by scaling theory, over restricted temperature and concentration ranges yields equivalent descriptions of the data. This ambiguity is due to the difficulty of discriminating between an exponential fit through the origin and a linear fit over a restricted data range if there is some scatter in the data. However, as no indication for a transition from a poor solvent to a good solvent regime is found, we conclude that excluded-volume effects are probably not important in the concentration–temperature region investigated here.

Autocorrelation functions of the scattered light contain a distribution of slow, q-independent modes beside a fast diffusive mode. The contribution of the slow modes decreases with increasing temperature and concentration in agreement with theoretical expectations. The exact origin of these modes is not known at present, but there is a marked similarity with the range of relaxation times obtained from dynamical mechanical measurements.

Values for an effective dynamic correlation length were calculated by using D_c obtained from the fast relaxation time. Corresponding values for the static correlation length were estimated from experimental values reported in the literature. For small values of ξ_s, ξ_e becomes proportional to ξ_s. For large values of ξ_s, ξ_e is clearly influenced by topological constraints in agreement with Brochard and de Gennes' theory and earlier experimental findings on Θ systems.

Acknowledgment. Support for this project from the Swedish Natural Science Council (NFR) is gratefully acknowledged. We thank Dr. M. Daoud, Dr. M. Delsanti, and Dr. E. Geissler for helpful discussions.

References and Notes

(1) de Gennes, P.-G. *Scaling Concepts in Polymer Physics*; Cornell University: London, 1979.
(2) Daoud, M.; Cotton, J. P.; Farnoux, B.; Jannink, G.; Sarma, G.; Benoit, H.; Duplessix, R.; Picot, C.; de Gennes, P.-G. *Macromolecules* **1975**, *8*, 804.
(3) Schäfer, L. *Macromolecules* **1984**, *17*, 1357.
(4) Wiltzius, P.; Haller, H. R.; Cannell, D. S.; Schaefer, D. W. *Phys. Rev. Lett.* **1983**, *51*, 1183.
(5) Štěpánek, P.; Persinski, R.; Delsanti, M.; Adam, M. *Macromolecules* **1984**, *17*, 2340.
(6) Cotton, J. P.; Nierlich, M.; Boué, F.; Daoud, M.; Farnoux, B.; Jannink, G.; Duplessix, R.; Picot, C. *J. Chem. Phys.* **1976**, *65*, 1101.
(7) Daoud, M.; Jannink, G. *J. Phys.* **1976**, *37*, 973.
(8) Moore, M. A. *J. Phys.* **1977**, *38*, 265.
(9) Okano, K.; Wada, E.; Kurita, K.; Hiramatsu, H.; Fukura, H. *J. Phys. Lett.* **1979**, *40*, L-171.
(10) Cherayil, B. J.; Kolodenko, A. L.; Freed, K. F. *J. Chem. Phys.* **1987**, *80*, 7204.
(11) Schaefer, D. W.; Joanny, J. F.; Pincus, P. *Macromolecules* **1980**, *13*, 1280.
(12) Schaefer, D. W.; Han, C. C. *Dynamic Light Scattering*; Pecora, R., Ed.; Plenum: New York and London, 1985; Chapter 5.
(13) Kinugasa, S.; Hayashi, H.; Hamada, F.; Nakajima, A. *Macromolecules* **1986**, *19*, 2832.
(14) Brochard, F.; de Gennes, P.-G. *Macromolecules* **1977**, *10*, 1157.
(15) Brochard, F. *J. Phys.* **1983**, *44*, 39.
(16) Nicolai, T.; Brown, W.; Johnsen, R.; Štěpánek, P. *Macromolecules* **1990**, *23*, 1165.
(17) Adam, M.; Delsanti, M. *Macromolecules* **1985**, *18*, 1760.
(18) Muthukumar, M.; Edwards, S. F. *Polymer* **1982**, *23*, 345.
(19) Weill, G.; des Cloizeaux, J. *J. Phys.* **1971**, *40*, 99.
(20) Akcasu, A. Z.; Han, C. C. *Macromolecules* **1979**, *12*, 276.
(21) Daoud, M.; Jannink, G. *J. Phys. Lett.* **1980**, *40*, 621.
(22) Adam, M.; Delsanti, M. *J. Phys.* **1980**, *41*, 731.
(23) Scholte, Th. G. *J. Polym. Sci., Part A-2* **1970**, *8*, 841.
(24) Brown, W.; Zhou, P.; Rymdén, R. *J. Phys. Chem.* **1988**, *92*, 6086.
(25) Brown, W. *Macromolecules* **1986**, *19*, 387, 1083.
(26) Yamakawa, H. *Modern Theory of Polymer Solutions*; Harper & Row: New York, 1974.
(27) Jakeš, J., to be published.
(28) Adam, M.; Delsanti, M. *J. Phys. (Paris)* **1984**, *45*, 1513.
(29) Okano, K.; Wada, E.; Kurita, K.; Fukuro, H. *J. Appl. Crystallgr.* **1978**, *11*, 507.
(30) Schmidt, M.; Burchard, W. *Macromolecules* **1981**, *14*, 210.
(31) Vink, H. *Eur. Polym. J.* **1974**, *10*, 149.
(32) Ichimura, T.; Okana, K.; Kurita, K.; Wada, E. *Polymer* **1987**, *28*, 1573.
(33) (a) Brown, W.; Nicolai, T.; Hvidt, S.; Štěpánek, S. *Macromolecules* **1990**, *23*, 357. (b) Nicolai, T.; Brown, W.; Hvidt, S.; Heller, K. *Macromolecules*, submitted.
(34) Roots, J.; Nyström, B. *Macromolecules* **1980**, *13*, 1595.
(35) Brown, W.; Mortensen, K. *Macromolecules* **1988**, *21*, 240.